

Theoretical and Practical Investigation of Stability Performance for Power Regulation in Hydroelectric Power Plants

Gökhan KAHRAMAN^{1*}, Erdem IŞIK¹

Highlights:

- A mathematical model of the power control system was created
- The transfer function of the system was calculated
- As a result of the calculations obtained under different operating conditions, ideal operating conditions were determined to minimize fluctuations in energy production.

ABSTRACT:

Hydroelectric power plants are the insurance of the interconnected system in order to provide fast energy to the system compared to other fossil fueled power plants. Hydroelectric power plants control the balance between the energy it supplies to the interconnected system and the pressurized water it uses with a system based on the fully automatic control principle. The quality of the energy supplied to the interconnected system depends entirely on this automatic control mechanism. In this study, mathematical models of the mechanisms that affect the automatic control system during the generation of energy in hydroelectric power plants are formed. Transfer functions of the obtained mathematical models are calculated by laplace transform. With the calculated transfer functions, the responses of the units of a hydroelectric power plant to the change of the amount of energy produced under different operating conditions are determined. The obtained data are compared with the actual conditions in a 1330 MW hydroelectric power plant with 8 Francis turbines. It is seen that the mathematical model and the turbine responses in real conditions are similar. In the calculations made at 115, 125, 135, 145 m. net head, the best stability conditions were obtained at 135 m. In addition, as a result of the calculations obtained under different operating conditions, ideal operating conditions are determined to minimize the fluctuations in energy production.

Keywords:

- Renewable Energy
- Hydroelectric Power Plants
- Automatic Control
- Mathematical Models
- Transfer Function

¹ Gökhan KAHRAMAN (Orcid ID: 0000-0002-8365-2447), Erdem IŞIK (Orcid ID: 0000-0003-4715-6582), Munzur University, Faculty of Engineering, Department of Mechanical Engineering, Tunceli, Türkiye

* Corresponding Author: Gökhan KAHRAMAN, e-mail: gokhankahraman@munzur.edu.tr

INTRODUCTION

There are various renewable and non-renewable energy sources in the world. Renewable energy sources are considered more environmental-friendly (Sharif et al., 2019). In hydroelectric power plants that are compatible with the interconnected system, power control is important. Because the quality of electricity produced depends entirely on power control (Ming et al., 2017; Wang et al., 2017; Weldcherkos et al., 2021). Power generation stability is still a major challenge to achieve the interconnected system objectives of renewable energy, and new challenges arise (Kundur et al., 1994). Low frequency oscillations related to the generation of hydroelectric energy have occurred in many regions such as Scandinavian power system (Weixelbraun et al., 2013), the Chinese Southern Power Network (Yinsheng, 2013) and the Turkish power system (Gencoglu et al., 2010). There are many studies in the literature about this problem of hydroelectric power plants. Guo and Yang have formulated the mathematical model of the system to investigate the stability performance for primary frequency regulation of the hydro turbine system with surge tank (Guo and Yang, 2018). Gonzalez et al. have conducted block-diagram and mathematical models for hydro-turbine systems and multi-hydro systems with balance flues and applied passivity-based control and stability analysis (Gonzalez et al., 2019; Gonzalez et al., 2020). Khodabakhshian and Hooshmand have designed a new PID control for hydroelectric power plants and examined the system's response to power changes (Khodabakhshian and Hooshmand, 2010). Yang et al. analyzed the hydraulic damping mechanism of low frequency oscillations in power systems using a non-linear hydroelectric power plant model (Yang, et al., 2018). Guo and Yang have made a model for frequency control in hydraulic turbines with balancers and examined the turbine's response to frequency changes (Guo and Yang, 2018). Shanab et al. compared the results produced by the Francis turbine experiment set in Al-Azhar University flow laboratory by measuring the response of the system to the change of values such as torque, flow and position of the wing (Shanab et al., 2020). Adhikari and Wood examined cross-flow hydraulic turbines by performing comparative analysis of partial load and flow control (Adhikari and Wood, 2018). Doolla et al. Proposed a load frequency control technique for an isolated small hydropower plant based on a multiple flow control system (Doolla et al., 2011). Sharma et al. (Sharma et al., 2018) designed an artificial neuro fuzzy inference system (ANFIS) based automatic power generation control (AGC) scheme for the hydro-turbine power system. Liu et al. Developed a model for performing load frequency control with dynamic valve position modeling for the hydro-thermal power system and developed an estimated fuzzy control method (Liu et al., 2016).

MATERIALS AND METHODS

Hydroelectric power plants transmit the potential energy of the pressurized water coming to the snail by means of forced pipes to the turbine wheel in the ratio of the opening gap to the turbine wheel and generate electricity by means of reverse electromotive force generated by the rotation of the generator connected to the turbine wheel by the shaft. It is important that the energy generated in the hydraulic turbines feeding the interconnecting systems is matched to the load demand in a timely manner, so that the network frequency always remains within a specified band, known as load-frequency control (Kundur et al., 1994). The quality of the energy supplied to the interconnected system depends entirely on the sensitivity of the load-frequency control. This regulator provides speed regulators which can be considered as the brain of hydroelectric power plants. The speed governors must be capable of responding to different operating conditions. This is a very difficult event as well as a necessary event for the quality of the energy produced. A properly functioning automatic control

system is required to evaluate and optimize the response of a turbine according to changing operating conditions. The control mechanism in a hydroelectric power plant is shown in Figure 1.

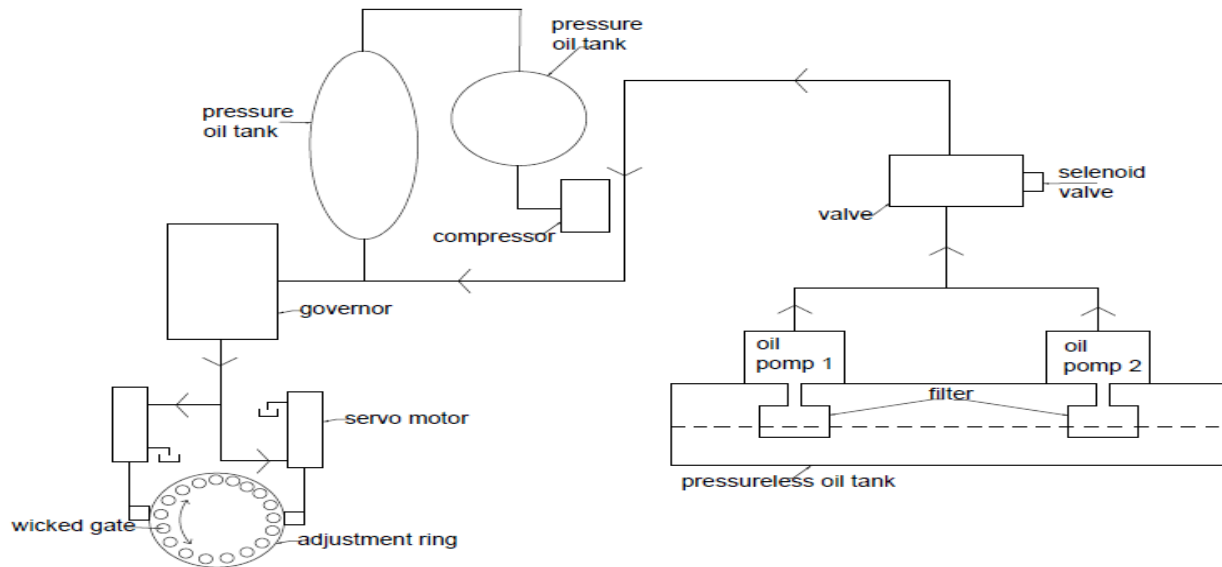


Figure 1. Adjustment blades control system in hydroelectric power plants

System shown in Figure 1 operates according to the principle of controlling the adjustment vanes with pressurized oil. The oil in the non-pressurized tank feeds the pressurized oil tank and the system by increasing the pressure with two screw-operated screw pumps. When the pressurized oil tank reaches a sufficient level, a switch shuts off the oil path by de-energizing the solenoid valve. In this process, the oil that will control the wings is supplied from the pressurized oil tank. The oil in the pressure oil tank is kept constant with compressed air according to the principle of incompressible fluids. The servomotors connected to the adjustment ring according to the up-regulation or down-regulation command of the speed governor open or close the wings. The opening position of the adjusting wings is transmitted to the speed governor by a feedback mechanism, thereby limiting the movement of the speed regulating main distribution valve.

Mathematical Modeling of Hydroelectric Power Plant

PID (proportional-integral-derivative) control is the most widely used control mechanism in hydroelectric power plants. This control can be applied mechanically, pneumatically and electrically. It provides precise control of the system. Equation 1 shows the PID control formula (Munoz-Hernandez et al. 2013)

$$u(t) = K_p \cdot e(t) + K_i \int_0^t e(t) dt + K_d \cdot \frac{d}{dt} e(t) \quad (1)$$

K_p represents the proportional gain, K_i represents integral gain and K_d represents the derivative gain. The formula given in Equation 2 and 3 shows the transfer function (TF) of the speed regulator in the "s" domain in a hydroelectric power plant connected to the interconnected system (Munoz-Hernandez et al., 2013)

$$TF_{Governor} = K_p + (K_i/s) + K_d \cdot s / (T_d \cdot s + 1) \quad (2)$$

$$K_p = 0.97 \cdot \frac{T_m}{T_w}, \quad K_i = 0.39 \cdot \frac{T_m}{T_w^2}, \quad K_d = 0.4 \cdot T_m \quad (3)$$

In Equation 3, "Tw" is the movement time parameter of water and Tm is the initial time parameter. The adjustment blades control the water flow to the turbine wheel. The position of the

control blades depends on the control signal of the speed regulator. Equation 4 gives the adjustment blades transfer function (Munoz-Hernandez et al., 2013).

$$TF_{\text{guide vane}} = \frac{Y(s)}{U(s)} = \frac{1}{(T_1.s+1).(T_2.s+1)} \quad (4)$$

T_1 and T_2 are time constants, which are determined by the pressure and flow characteristics of the servomotor and the adjustment blade. $Y(s)$ speed regulator output signal $U(s)$ is the feedback signal from the adjustment blades to the speed regulator.

There are two servomotors in the hydraulic turbines and they control the adjustment blades with the pressurized oil coming from the speed regulator main distribution valve. Equation 5 shows the servomotor transfer function.

$$TF_{\text{servo}} = \frac{1}{s.Tp+1} \quad (5)$$

The mathematical modeling of the penstock of a hydroelectric power plant is determined by three basic equations: water velocity in the penstock, gravity effect and power generation in the turbine. Equation 6 and 7 shows the penstock pipe transfer function.

$$TF_{\text{penstock}} = \frac{1-s.Tw}{1+0,5.s.Tw} \quad (6)$$

$$T_w = \frac{L.q}{h.g.A} \quad (7)$$

In Equation 7, "L" is the penstock length, "q" is the penstock water flow rate, "h" is the net head, "g" is the gravitational acceleration and "A" is the penstock pipe cross-sectional area.

The generator dynamics is represented by the oscillation equation that relates the rotating machine inertia (T_m) to the acceleration torque. The load depends on the D value of the load damping. Equation 8 shows the turbine-generator transfer function (Kundur et al., 1994).

$$TF_{\text{turbine-generator}} = \frac{1}{s.Tm+D} \quad (8)$$

Block diagram of hydroelectric power plant model

Hydroelectric power plant in this research model is on the Fırat River in the east of Türkiye. The total installed capacity of the plant is 1330 MW and the installed capacity is achieved with 8 turbine-generator unit. Penstock pipes of hydraulic turbines are not shared. Each hydraulic turbine has a penstock pipe coming from the upstream side. Figure 2 shows a block diagram designed for a turbine of a hydroelectric power plant.

Table 1. Values used in calculations

L1	1. Turbine penstock length	512.739 m
L2	2. Turbine penstock length	516.057 m
L3	3. Turbine penstock length	520.037 m
L4	4. Turbine penstock length	524.626 m
L5	5. Turbine penstock length	529.919 m
L6	6. Turbine penstock length	535.774 m
L7	7. Turbine penstock length	545.346 m
L8	8. Turbine penstock length	548.684 m
Q	The water flow passing from the penstock	95-105-115-125-135 m ³ /s
H	Net head	105-115-125-135-145 m
G	Gravity acceleration	9.81 m/s ²
A	Sectional area of the penstock	21.2 m ²
T _w	Water starting time of a single penstock	Calculated
T _p	Pilot valve servomotor time constant	0.05 s
T _m	Machine starting time	7.99 s
D	Load damping factor	0.5

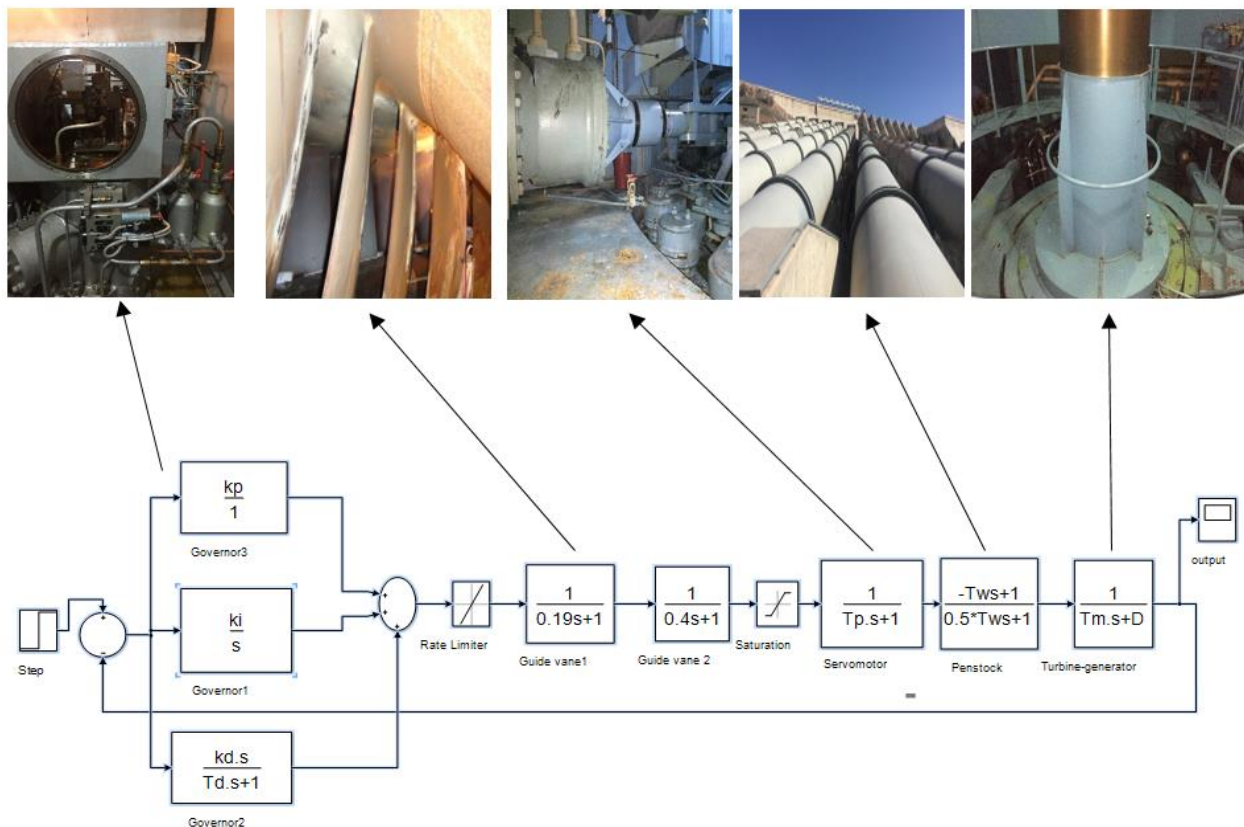


Figure 2. Hydroelectric Power Plant Block Diagram

The transfer function calculated according to the block diagram in Figure 2 is given in Figure 3.

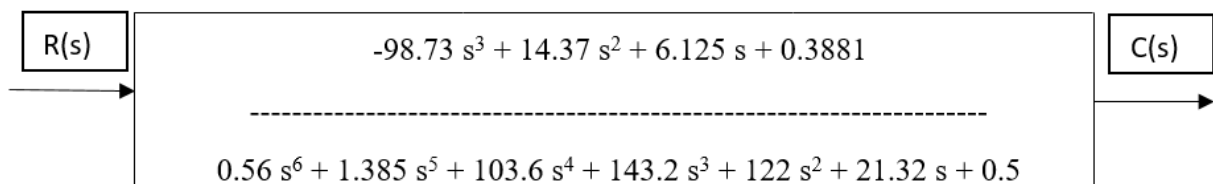


Figure 3. Transfer Function Calculated for Hydroelectric Power Plant

A description of the terms used in the calculations according to the block diagram in Figure 2 and the used values are shown in Table 1.

RESULTS AND DISCUSSION

In the block diagram, the responses of the turbine-generator units to load exchange under different operating conditions are obtained graphically by using the actual values of the hydroelectric power plant. In the sampled hydroelectric power plant, the lengths of the penstock to each turbine are different. The transfer function calculated according to the penstock lengths of each unit is shown in Figure 4.

In the graph of Figure 4, when the transfer functions obtained at different time periods of 20 seconds at different penstock lengths are examined, no significant change is observed in the reactions of the units. In the penstock lengths used in the calculations, the difference between the shortest penstock and the longest penstock is approximately 36 m at a distance of 36 m, the response of the units is not significantly affected

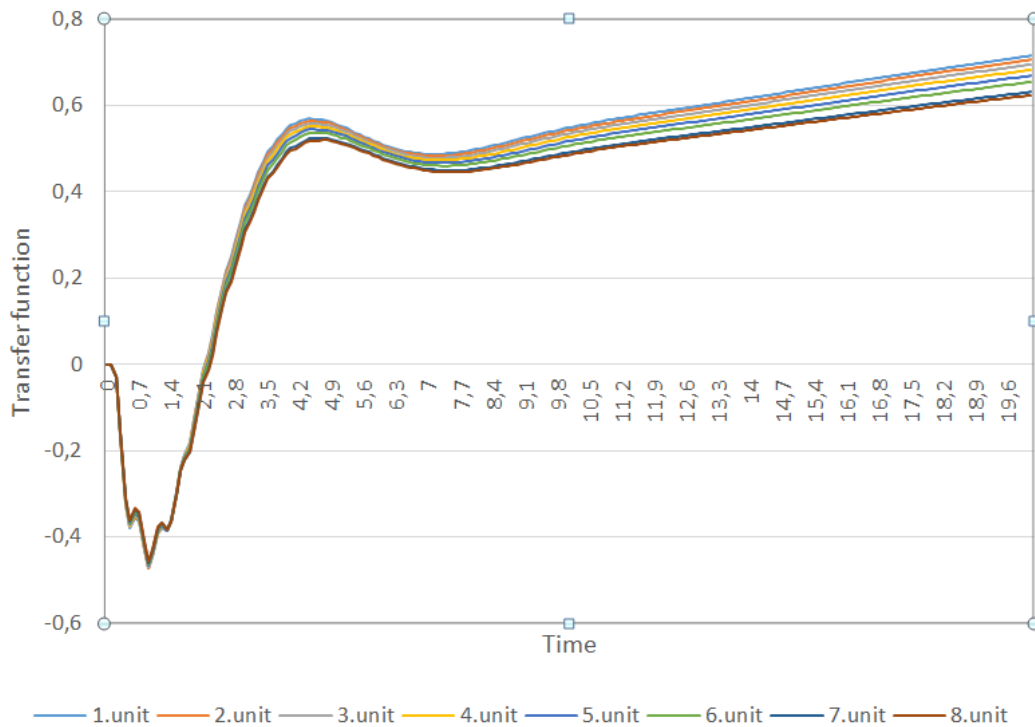


Figure 4. Time-transfer function graph based on the penstock lengths of different units

Figure 5 shows the change of transfer function at different flow rates to the turbine.

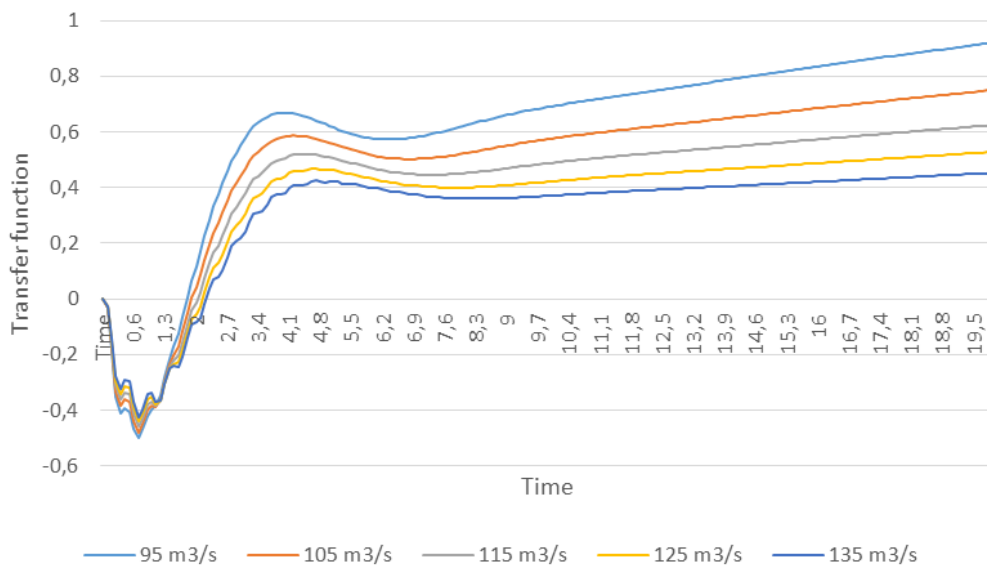


Figure 5. Variation of transfer function over time at different flow rates

In the graph in Figure 5, the transfer function is calculated according to the maximum minimum and average values that can pass through a turbine. As it can be seen from the graph, maximum oscillation occurs in the energy produced at a flow rate of $135 \text{ m}^3 \text{ s}^{-1}$. At $95 \text{ m}^3 \text{ s}^{-1}$ flow rate, minimum oscillation occurs. It is also seen from the graph that as the amount of flow to the turbine decreases, the time to reach the target energy produced decreases.

Figure 6 shows the transfer function graphs obtained at different hydraulic head.

As shown in Figure 6, the oscillation in energy production is at highest in 115 m hydraulic head and it is at least in 135 m hydraulic head. This shows us that the best control is realized in the middle

heads. Pressure fluctuations at very high (145 m) and very low head (115 m, 125 m) negatively affect the control.

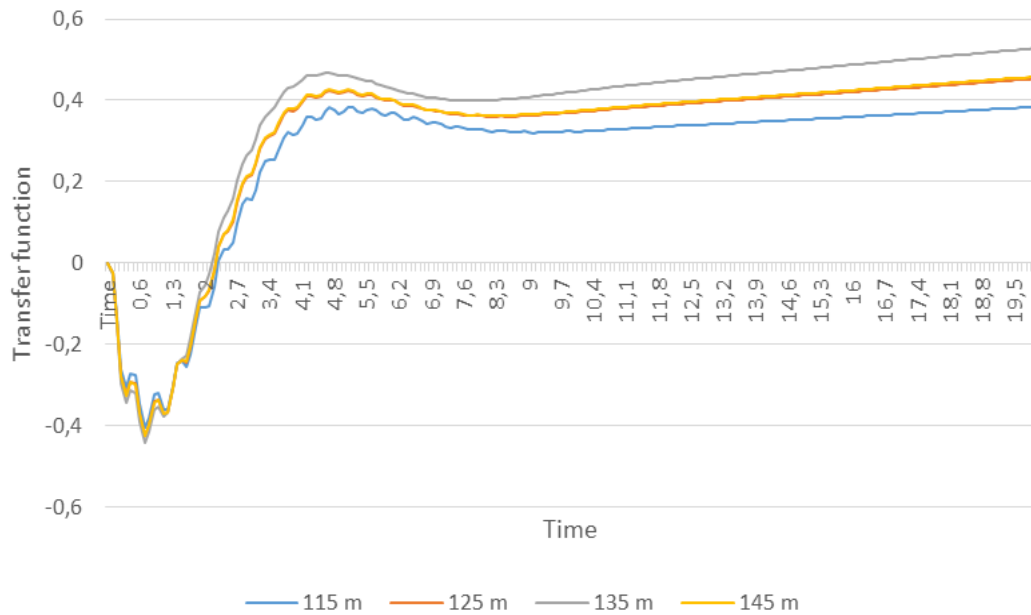


Figure 6. Time-varying transfer function at different hydraulic head

In addition, it is seen that the time to reach the target load is shorter in 135 m hydraulic head.

The graphs in Figures 7 and 8 show the power generated against the time generated in a turbine-generator unit of the hydroelectric power plant described above.

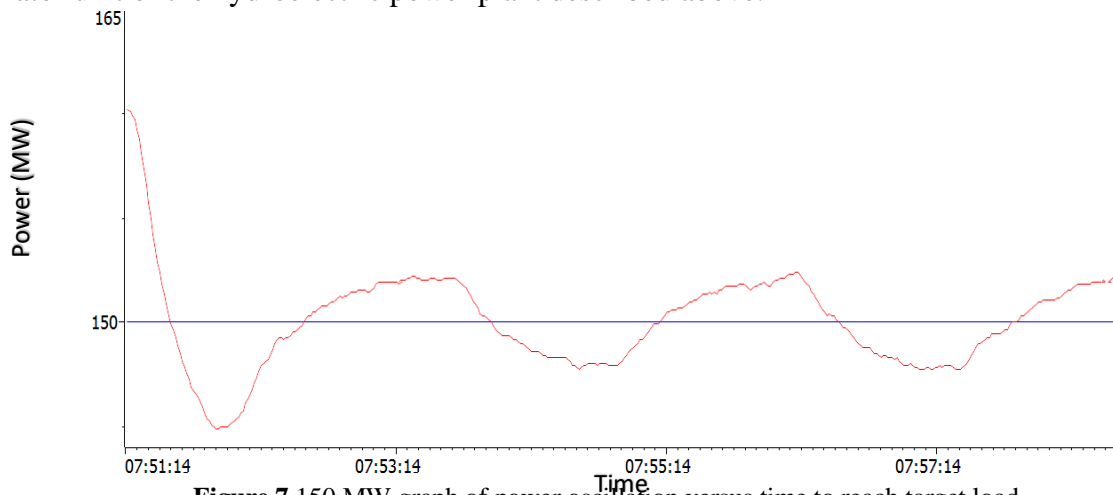


Figure 7. 150 MW graph of power oscillation versus time to reach target load

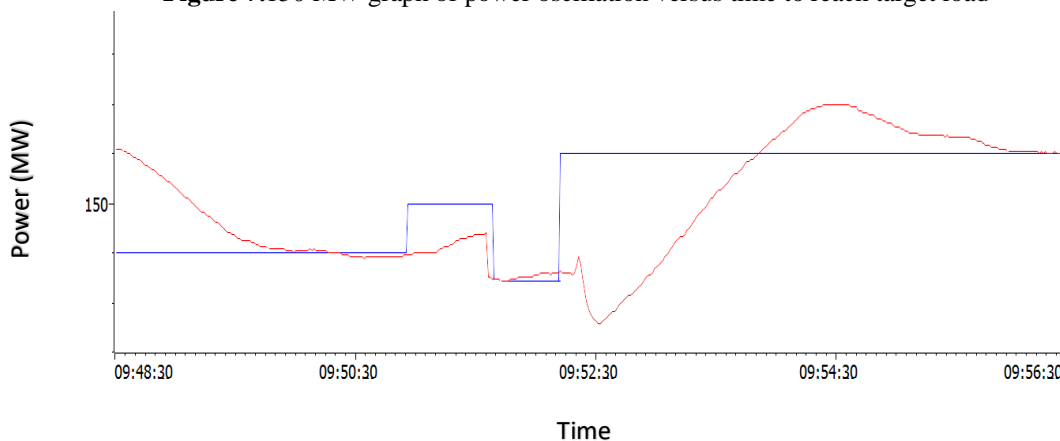


Figure 8. Graph of power oscillation versus time to achieve different target loads

The graphs in Figures 7 and 8 are measured from a real turbine-generator unit. The x-axis of the graphs shows the time at which the measurement is made.

In the graph in Figure 7, a target load of 150 MW is given and the unit is followed while it captures this load. The power oscillations when the unit captures the target load are similar to the transfer function graphs in Figures 4, 5 and 6. In the graph in Figure 8, different load targets are given to the unit and the response of the units over time is measured. The actual response of the system at different load targets is similar to that of the calculated transfer function.

The graph in Figure 9 shows the theoretical and practical responses of the unit when reaching a target load of 151 MW.

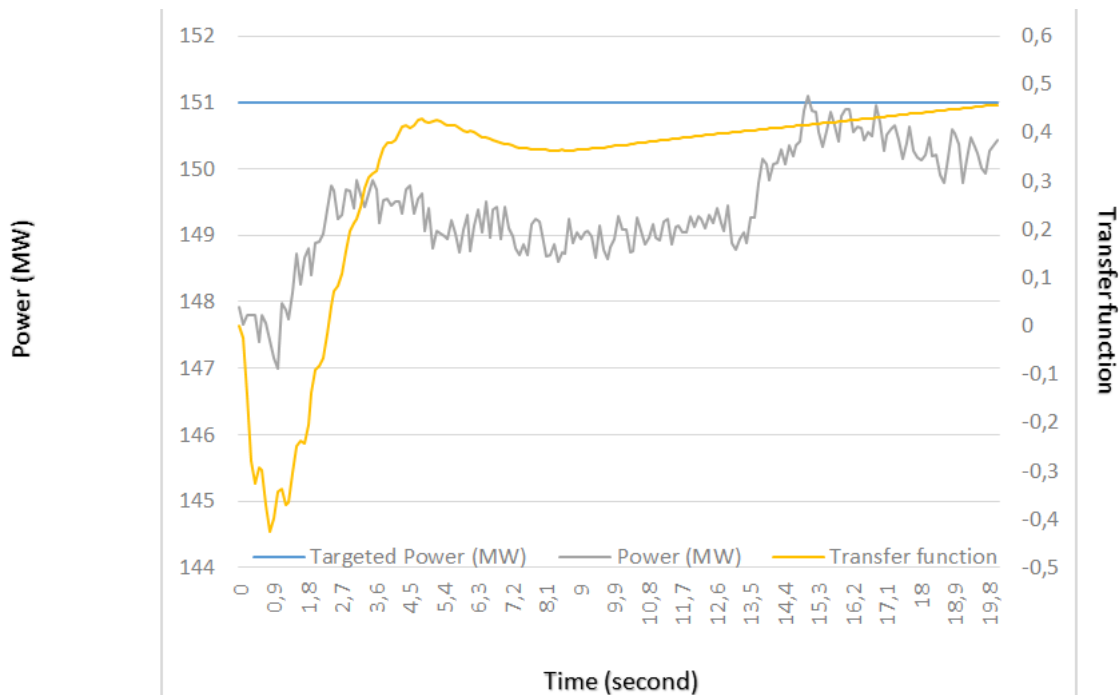


Figure 9. The theoretical and practical responses of the unit to the determined target load

As shown in Figure 9, when the unit reaches a target load of 151 MW, the response of the transfer function obtained as a result of the model is similar to the response of the unit under real conditions.

CONCLUSION

The results obtained in the study are given below.

- Transfer function of the hydroelectric power plant with 8 Francis turbines of 1330 MW power has been calculated by creating block diagram. With the calculated transfer function, the responses of the turbine generator units to the change of energy production have been determined for different penstock lengths, different turbine flow rates and different hydraulic head. The operating conditions at which the optimum load oscillation occurs are determined.

- The actual turbine-generator units have been given target loads during energy production and their responses to reach these target loads have been measured against time.

- At the end of the study, the target load of 151 MW has been determined and the theoretical and practical responses of the turbine-generator unit have been observed over time. The theoretical and practical responses are found to be similar in the same time periods.

- The responses of the unit in reality can be brought closer to the response of the calculated transfer function by making the ideal PID control or speed regulator pressure oil adjustment.

This study is surveyed for hydroelectric power plants operating to the interconnected system, will contribute to give higher quality energy to the system.

ACKNOWLEDGEMENTS

Conflict of Interest

The article authors declare that there is no conflict of interest between them.

Author's Contributions

The authors declare that they have contributed equally to the article.

KAYNAKLAR

- Adhikari, R.C. and Wood, D.H. (2018). Computational analysis of part-load flow control for crossflow hydro-turbines. *Energy for Sustainable Development* 45:38-45. <https://doi.org/10.1016/j.esd.2018.04.003>
- Doolla, S., Bhatti, T.S., and Bansal, R.C. (2011). Load Frequency Control of an Isolated Small Hydro Power Plant Using Multi-pipe Scheme. *Electric Power Components and Systems* 39. <https://doi.org/10.1080/15325008.2010.513362>
- Gencoglu, C., Tor, O.B., Cebeci, E., Yilmaz, O., and Guven, A.N. (2010). Assessment of the effect of hydroelectric power plants' governor settings on low frequency inter area oscillations. *In: International conference on power system technology (POWERCON)*. IEEE.
- Gonzalez, W.G., and Garces, A. (2019). Escobar A., Passivity-based control and stability analysis for hydro-turbine governing systems. *Applied Mathematical Modelling* 68:471-486. <https://doi.org/10.1016/j.apm.2018.11.045>
- Gonzalez, W.G., and Montoya, O.D. (2020). Garces A., Standard passivity-based control for multi-hydro-turbine governing systems with surge tank. *Applied Mathematical Modelling* 79:1-17. <https://doi.org/10.1016/j.apm.2019.11.010>
- Guo, W., and Yang, J. (2018). Modelling and dynamic response control for frequency regulation of hydro turbine governing system with surge tank. *Renewable Energy* 121:173-187. <https://doi.org/10.1016/j.renene.2018.01.022>
- Guo, W., and Yang, J. (2018). Stability performance for primary frequency regulation of hydro-turbine governing system with surge tank. *Applied Mathematical Modelling* 54:446-466. <https://doi.org/10.1016/j.apm.2017.09.056>
- Khodabakhshian, A., and Hooshmand, R. (2010). A new PID controller design for automatic generation control of hydro power systems. *Electrical Power and Energy Systems* 32:375-382. [10.1016/j.ijepes.2009.11.006](https://doi.org/10.1016/j.ijepes.2009.11.006)
- Kundur, P., Balu, N.J., and Lauby, M.G. (1994). Power system stability and control. New York: McGraw-Hill.
- Liu, X., Kong, X., and Lee, K. (2016). Distributed model predictive control for load frequency control with dynamic fuzzy valve position modelling for hydro-thermal power system. *IET Control Theory and Applications*. 10. 2016. [10.1049/iet-cta.2015.1021](https://doi.org/10.1049/iet-cta.2015.1021).
- Ming, B., Liu, P., Guo, S., Zhang, X., Feng, M., and Wang, X. (2017). Optimizing utility-scale photovoltaic power generation for integration into a hydropower reservoir by incorporating long- and short-term operational decisions. *Appl Energy* 204:432-45.
- Munoz-Hernandez, G.A., Mansoor, S.P., and Jones, D.L. (2013). Modelling and Controlling Hydropower Plants. *Springer*. Doi [10.1007/978.1.4471.2291.3](https://doi.org/10.1007/978.1.4471.2291.3)

- Shanab, B.H., Elrefaie, M.E., and El-Badawy, A.A. (2020). Active control of variable geometry Francis Turbine. *Renewable Energy* 145:1080-1090. <https://doi.org/10.1016/j.renene.2019.05.125>
- Sharif, A., Raza, S.A., Ozturk, I., and Afshan, S. (2019). The dynamic relationship of renewable and nonrenewable energy consumption with carbon emission: A global study with the application of heterogeneous panel estimations. *Renewable Energy* 133:685-691. <https://doi.org/10.1016/j.renene.2018.10.052>
- Sharma, G., Nasiruddin, I., Niazi, K.R., and Bansal, R.C. (2018). ANFIS Based Control Design for AGC of a Hydro-hydro Power System with UPFC and Hydrogen Electrolyzer Units. *Electric Power Components and Systems* 46:2018. <https://doi.org/10.1080/15325008.2018.1446197>
- Wang, W., Li, C., Liao, X., and Qin, H. (2017). Study on unit commitment problem considering pumped storage and renewable energy via a novel binary artificial sheep algorithm. *Appl Energy* 187:612–626.
- Weixelbraun, M., Renner, H., Kirkeluten, O., and Lovlund, S. (2013). Damping low frequency oscillations with hydro governors. IEEE PowerTech (POWERTECH). Grenoble.
- Weldcherkos, T., Salau, A.O., and Ashagrie, A. (2021). Modeling and design of an automatic generation control for hydropower plants using Neuro-Fuzzy controller. *Energy Reports* 7:6626-6637. <https://doi.org/10.1016/j.egy.2021.09.143>
- Yang, W., Norrlund, P., Bladh, J., Yang, J., and Lundin, U. (2018). Hydraulic damping mechanism of low frequency oscillations in power systems: Quantitative analysis using a nonlinear model of hydropower plants. *Applied Energy* 212:1138-1152. <https://doi.org/10.1016/j.apenergy.2018.01.002>
- Yinsheng, S.U. (2013). Analysis on the CSG's power oscillation events in recent years (in Chinese). *Southern Power Syst Technol.* 7:54–7.